

# Performance Prediction of Air-conditioning Systems Based on Fuzzy Neural Network



Ye Xia<sup>1</sup>, Mao-Hsiung Hung<sup>2\*</sup>, Rong Hu<sup>2</sup>

<sup>1</sup> Key Laboratory of New Energy and Energy-saving in Building, Fujian University of Technology, Fuzhou 350118, China

<sup>2</sup> Fujian Province Key Laboratory of Automotive Electronics and Electric Drive, Fujian University of Technology, Fuzhou 350118, China  
2751808409@qq.com, {mhhung, hurong}@fjut.edu.cn

Received 11 November 2016; Revised 27 January 2017; Accepted 30 March 2017

**Abstract.** This study developed a Fuzzy neural network (FNN) model for air-conditioning system of a passenger car to predict the cooling capacity, compressor power input and the coefficient of performance (COP) of the automotive air-condition (AAC) system. We developed an experimental rig to generate required data. The experimental rig is demanded a steady state under several changing conditions such as compressor speed, air temperature of evaporator inlet, air temperature of condenser inlet and air velocity of evaporator inlet. A computer simulation has been conducted. The simulation results of the FNN are compared with the experimental results of the rig. The result comparison indicates that our proposed FNN model performs high accuracy prediction for automotive air-conditioning systems.

**Keywords:** air-condition system, fuzzy neural network, performance prediction

## 1 Introduction

The analysis of the performance and operational strategies of Heating Ventilation and Air Conditioning (HVAC) systems becomes very important for the effective usage of energy [1]. HVAC systems to improve the performance have been discussed over classical control [2-3]. The techniques include expert systems, neural networks, fuzzy logic, and genetic algorithm. Automotive air-conditioning (AAC) system is used to maintain comfortable condition in the compartment of passenger cars. To achieve such condition, the panel outlet for airflow direction, velocity, volume and temperature has to be adjustable over a large range of climatic and driving conditions. The compressor of the AAC systems is belt driven by the engine hence its speed is directly governed by the engine speed and causes the cooling capacity of the system to vary with the engine speed. The AAC system must need to have capable of lowering the air temperature in the passenger compartment quickly and quietly. These conditions make it complicated to analyze the AAC systems compared to that of the stationary air-condition systems, as described by Kargilis [4].

Traditionally, the performance of an AAC system has been done experimentally by many researchers such as Rubas and Bullard [5] on determination of COP of refrigerant cycle for AAC system, Ratts and Brown [6] on effects of the R-134a refrigerant charge level on the performance of the AAC system, A1-Rabghi and Niyaz [7] on COP determination using two types of refrigerants, R-12 and R-134a, as a function of compressor speed and Kaynakli [8] on determination of optimum operating conditions for AAC system using refrigerant R-134a. Hosoz [9] carried out experimental work on an AAC system operating in both air-conditioning and heat pump modes, with varying compressor speed and air temperatures at the inlets of both outdoor and indoor coils.

ANN has been proven to be a useful tool in modeling in refrigeration and air-conditioning system for

---

\* Corresponding Author

performance consumption [10]. Chang [11] studied on relationship of power consumption, chilled water temperature and cooling water temperatures of chillers in air-conditioning system. Ertunc [12] applied both ANN and adaptive neuron-fuzzy inference system (ANFIS) models to predict performance of evaporative condenser such as the heat rejection rate, temperature of the leaving refrigerant along with dry and wet bulb temperature of the leaving air stream. A complete review on application of ANN for energy and energy analysis of refrigeration, air conditioning and heat pump systems has been done by Mohanraj et al. [13]. Recently, Abdel-Hanmid [14] investigated fuzzy logic control of the air conditioning system of building for efficient energy operation and comfortable environment. Ning Li [15] reported an ANN-based on-line adaptive controller to control indoor air temperature and humidity simultaneously within the entire expected controllable range by varying compressor and supply fan speeds.

Although there has been many researchers of ANN applications in air-conditioning system, quite a few studies being done on AAC with fuzzy neural network. It is well known that Fuzzy neural network (FNN), which incorporates the advantages of fuzzy inference and neuron learning, has been exploited by many researchers. In this study, FNN model for an automotive air-conditioning (AAC) system was developed which employs a vapor-compression circuit working with refrigerant R-134a. The model was developed using several steady-state input data of the AAC system obtained from the actual experiments. The presented FNN model is then used to predict the AAC system performance namely cooling capacity of the evaporator, the input power to the compressor and the coefficient of performance (COP) of the AAC system. The result values to the real experimental data are compared. The comparison indicates that our proposed FNN model performs high accuracy prediction for automotive air-conditioning systems.

The remainder of this paper is organized as follows. We reviewed several related works in Section 2. Section 3 describes fuzzy neural networks, which includes structure of FNN, generation of fuzzy rule, parameter adjustment and summary of FNN. In Section 4 and 5, we describe the proposed FNN model of AAC system and the model validation. In Section 6 and 7, we describe our experiments, and then demonstrate the performance evaluation of the proposed model and discuss the experimental results. The conclusions are drawn in Section 8.

## 2 Related Works

In order to fulfill the demand for fuel saving and energy efficiency, automotive industry face a great challenge posed by the reinforcement of more environmental regulations. The manufactures are concerned with the design of a more efficient AAC system because the air conditioner compressor is the single largest auxiliary load on an automobile engine [21].

A conventional AAC system runs with its compressor belt driven by a combustion engine. During partial load condition, the compressor is cycled on-off via engagement and disengagement of a magnetic clutch to maintain the demanded cooling capacity during partial load condition. This kind of control method has a drawback that the energy loss associated with the pressure equalization during compressor stoppage, friction losses due to the pulley belt mechanism and poor cooling performance.

For an air conditioning system, the reduction in power consumption can be achieved by converting the control strategy from the conventional compressor on-off cycling to a variable speed operating mode [22-23]. Energy saving can be achieved because the establishment of a proper speed control of the variable speed compressor (VSC) can insure a continuous matching between the varying thermal load and the cooling capacity [24]. Furthermore, compared to the fixed speed operation, variable speed operation can deliver better temperature control and faster response to sudden change in thermal load. This control method is widely used in heavy trucks, buses, electric vehicles, in which high voltage battery supply is available. Recently, this method become a prospective application in conventional vehicles, as the key German carmakers are working on the stepping up of the current 12 V power supply to the proposed 48 V power net system [25]. This transition will facilitate to integrate an electric VSC in the conventional vehicle powered fully by the 48 V battery.

Considering the promising improvement brought about by the VSC application, several controllers for VSC have been proposed in the literature. The literature [22, 26-27] reported about that the implementation of proportional-integral and derivative (PID) control in regulating the compressor speed of an air conditioning system. However, because the inherently nonlinear dynamic behavior of the air conditioning system [28], a simple PI/PID controller with fixed control parameters can be used to

consistently deliver optimal control performance over the wide range of operating conditions.

Some literatures [29-30] reported linear model based controller for an air conditioning system. A detailed nonlinear physical model of the vapor compression cycles derived from first principle are preliminary required to back up the controller design in the proposed control methods [31-32]. However, it is a challenging task to de-velop an adequate physical model with satisfactory prediction accuracy, because the physical system is highly nonlinear and there are complex interconnections between the subsystems that mutually influence one another.

Artificial neural network (ANN) has been well-known for its capability as a universal approximator to fit nonlinear dynamic system without prior physical knowledge of the plant [33-34]. Artificial intelligence is a state-of-the-art technology that resembles the human thinking process in decision making and strategy learning, and it has been well recognized for its outstanding ability in controlling complex systems. The ANN and fuzzy logic are two effective tools in developing an intelligent control engineering model. This study is based on a rule base, fuzzy control, and counter propagation neural network establish a model for automotive air condition pre-diction system.

### 3 Fuzzy Neural Networks

#### 3.1 Structure of FNN

Generally, a wide class of MIMO nonlinear dynamic systems can be represented by the nonlinear discrete model with an input-output description form [16]:

$$y(n) = \mathbf{f}[y(n-1), y(n-2), \dots, y(n-k+1); \mathbf{u}(n), \mathbf{u}(n-1), \dots, \mathbf{u}(n-p+1)] \quad (1)$$

where  $y$  is a vector containing  $m$  system outputs,  $\mathbf{u}$  is a vector of system inputs;  $\mathbf{f}$  is a nonlinear vector function, representing  $m$  hyper surfaces of the system, and  $k, p$  is the maximum lag of the output and input respectively.

Selecting  $[y(n-1), \dots, y(n-k+1); \mathbf{u}(n), \mathbf{u}(n-1), \dots, \mathbf{u}(n-p+1)]$  as the fuzzy network's input and  $y(n)$  the fuzzy network's output,  $x_n, y_n$  at time  $t$ , the above equation can be put as

$$y_n = \mathbf{f}(x_n) \quad (2)$$

The aim of the new FNN algorithm is to approximate  $\mathbf{f}$  such that

$$\hat{y}_n = \hat{\mathbf{f}}(x_n) \quad (3)$$

where  $\hat{y}$  is the output of FNN. The objective is to minimize the error between the system output and the actual output  $\|y_n - \hat{y}_n\|$ . The structure of FNN illustrated by Fig. 1 consists of five layers to realize the following fuzzy rule model:

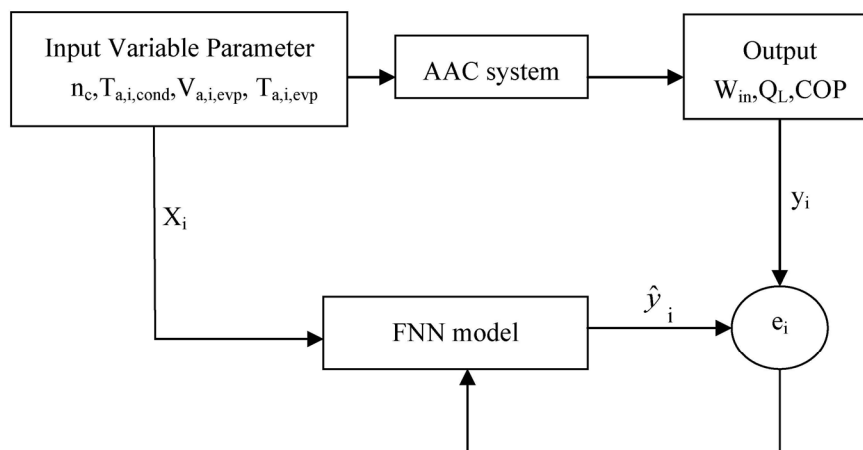


Fig. 1. FNNs model representation of the AAC system

If  $(x_1 \text{ is } A_{1k}) \text{ AND } (x_2 \text{ is } A_{2k}) \text{ AND } \dots \text{ AND } (x_r \text{ is } A_{rk})$ ,  
 then  $(y_1 \text{ is } a_{1k}) \dots (y_m \text{ is } a_{mk})$   
 where  $a_{jk} (j=1,2,\dots,m, k=1,2,\dots,u)$  is a constant parameter in rule  $k$ ,  $A_{ik} (i=1,2,\dots,r)$  is the membership value of the input variable  $x_i$  in rule  $k$ ,  $r$  is the dimension of the input vector  $\mathbf{x} (\mathbf{x} = [x_1, \dots, x_r])$ ,  $u$  is the number of fuzzy rules,  $m$  is the dimension of the output vector  $\hat{y} (\hat{y} = [\hat{y}_1, \dots, \hat{y}_m])$ . In FNN, the number of fuzzy rules  $u$  changed. Initially, there is no fuzzy rule and then they are added and removed during learning.

### 3.2 Generation of Fuzzy Rule

**The significance concept for a rule.** For a RBD network with  $u$  neurons, the output is given by

$$\hat{y} = \sum_{k=1}^u R_k(x) a_k \quad (4)$$

while  $\hat{y} = [\hat{y}_1, \hat{y}_2, \dots, \hat{y}_m]^T$ ,  $a_k = [a_{1k}, a_{2k}, \dots, a_{mk}]^T$ ,  $R_k(x)$  represents the  $k$ -th hidden neuron for an input vector  $\mathbf{x} \in \mathfrak{R}^r$

$$R_k(x) = \exp\left(-\frac{\|\mathbf{x} - \mu_k\|^2}{\sigma_k^2}\right) \quad (5)$$

$a_k$  is the connecting weight between 3rd layer and 4rd, and are the center and width of the  $k$ -th hidden neuron, respectively,  $k=1,\dots,u$ . The algorithm introduces the conception of influence based on overall inputs contributing to the hidden neurons so far.

On line learning, a series of training samples  $(x_i, y(x_i))$ ,  $i=1,2,\dots$  are randomly drawn and presented one by one to the system. In air condition system these input samples  $x_i$  have a uniform distribution. Assume a RBF network with  $K$  neurons has been reached after  $n$  input observers. The network output for an input  $X$  is given by

$$\hat{y}_1 = \sum_{j=1}^K a_j R_j(x_i) \quad (6)$$

If the neuron  $k$  is removed, the output of the RBF network with the remaining  $k-1$  neurons is

$$\hat{y}_2 = \sum_{j=1}^{k-1} a_j R_j(x_i) + \sum_{j=k+1}^K a_j R_j(x_i) \quad (7)$$

Thus, for an observation  $X$ , the error resulting  $E$  after removing neuron  $k$  is the absolute difference between  $\hat{y}_1$  and  $\hat{y}_2$ ; given by

$$E(k, i) = |\hat{y}_1 - \hat{y}_2| = |a_k| R_k(x_i) \quad (8)$$

Using the significance concept, the influence of the  $k$ -th fuzzy rule as its statistical contribution to the overall output of FNN is given by

$$C(k, i) = |a_k| \frac{R_k(x_i)}{\sum_{k=1}^K R_k(x)} \quad (9)$$

**Learning algorithm.** The leaning algorithm of FNN consists of two aspects: determination the number of fuzzy rules and adjustment of the parameters of fuzzy rules named neurons. In this work, the neurons should be automatically added and removed.

A FNN begins with no fuzzy rules. As inputs  $x_n, y_n$  ( $n$  is the time index) are received sequentially during learning, growing of fuzzy rules is based on the following two conditions.

(1) System error: when the  $k$ th observation arrives, the system error is calculated as follows

$$e_n = \|y_i - \hat{y}_i\| \quad (10)$$

Whether a new rule is added, the system error should be considered.

(2) Accommodation boundary: The accommodation criterion is described as follows: for the  $i$ th observation  $(\mathbf{x}_i, y_i)$ , calculate the distance  $d_i(j)$  between the observation  $x_i$  and the center  $u_j$  of an existing RBF unit, i.e.,

$$d_i(j) = \|\mathbf{x}_i - u_j\| \quad j = 1, 2, \dots, u \quad (11)$$

Here  $u$  is the number of existing fuzzy neurons.

$$\text{If } d_{\min} > k_d, \text{ then find } d_{\min} = \arg \min(d_i(j)) \quad (12)$$

A rule should be added to reduce the error of predication. Otherwise, the observation  $(\mathbf{x}_i, y_i)$  can be represented perfectly by the existing nearest RBF unit, and no need to add a new neuron. Here,  $k_d$  is the effective radius of accommodation boundary.

$$k_d = \max(d_{\max} \times r^i, d_{\min}) \quad (13)$$

$d_{\max}$  is the largest length of input space,  $d_{\min}$  is the smallest length of interest, and  $r$  is the decay constant.

Growing of fuzzy rules is based on the following two criteria which the distance criterion and the influence of the new added fuzzy rule  $u+1$  :

$$\begin{aligned} d_{\min} > k_d \\ E(\mathbf{x}_i, u+1) = \left| a_{u+1} \frac{R_{u+1}(x_i)}{\sum_{k=1}^{u+1} R_k(x_i)} \right| > e_g \end{aligned} \quad (14)$$

$e_g$  is the distance threshold.

When the fuzzy rule  $u+1$  is added, its corresponding antecedent and consequent parameters are allocated as follows:

$$\begin{aligned} a_{u+1} &= e_n, \\ \mu_{u+1} &= \mathbf{x}_n, \\ \sigma_{u+1} &= k \times d_{\min} \end{aligned} \quad (15)$$

### 3.3 Parameter Adjustment

In this FNN, all parameters are justified not similar to the work done by [20], which only the parameters related with winner rule are updated by the EKF algorithm.

When no neurons are added, the network parameter vector  $\theta$ , ( $\theta_k = [\theta_1, \theta_2, \dots, \theta_u]^T = [a_1, \mu_1, \sigma_1, \dots, a_u, \mu_u, \sigma_u]^T$ ) is updated by

$$\theta_k = \theta_{k-1} + e_k k_k \quad (16)$$

where  $k_k$  is the Kalman gain vector given by

$$k_k = [N_k + B_k^T P_{k-1} B_k]^T P_{k-1} B_k \quad (17)$$

And  $B_n$  is the gradient vector which has the following form

$$B_k = [R_1(x_k), R_1(x_k) \frac{2a_1}{\sigma_1^2} (x_k - \mu_1)^T, R_1(x_k) \frac{2a_1}{\sigma_1^3} \|x_k - \mu_1\|^2, \dots, R_u(x_k), R_u(x_k) \frac{2a_u}{\sigma_u^2} (x_k - \mu_u)^T, R_u(x_k) \frac{2a_u}{\sigma_u^3} \|x_k - \mu_u\|^2]^T \quad (18)$$

Here,  $N_k$  is the variance of the measurement noise and  $P_k$  the error covariance matrix which is updated by

$$P_k = [I - k_k B_k^T] P_{k-1} + Q_0 I \quad (19)$$

Where  $Q_0$  is a scalar which determines the allowed random step in the direction of gradient vector and  $I$  the identity matrix. When a new hidden neuron is allocated, the dimensionality of  $P_k$  increases to

$$P_k = \begin{bmatrix} P_{k-1} & 0 \\ 0 & P_0 I \end{bmatrix} \quad (20)$$

where  $x$  is an estimate of uncertainties in the initial values assigned to the parameters. The dimension of the identify matrix  $e_i$  is equal to the number of new parameters introduced by new hidden units.

When the first observation  $y_i$  arrives, some initializations are conducted since there are no hidden neurons at the beginning of the learning process. We have the first rule  $\hat{y}_i$ , where  $n_c, T_{a,i,cond}, V_{a,i,evp}, T_{a,i,evp}$  is the pre-established constant.

### 3.4 Summary of FNN

Given the growing and pruning thresholds  $x$ , for each observation  $\hat{y}_i$ , where  $y_i$  and

$$A_{ik}(x) = \exp\left(-\frac{(x_i - \mu_{ik})^2}{\sigma_k^2}\right) \quad k=1,2,\dots,u \text{ do}$$

(1) Compute the system output:

$$\hat{y}_n = \frac{\sum_{k=1}^u a_k R_k(x_n)}{\sum_{k=1}^u R_k(x_n)}$$

$$R_k(x_n) = \exp\left(-\frac{1}{\sigma_k^2} \|x_n - \mu_k\|\right)$$

(2) Calculate the parameters required in the growth criterion:

$$d_i(j) = \|x_i - u_j\| \quad j=1,2,\dots,u ; d_{\min} = \arg \min(d_i(j)) ;$$

$$e_n = \|y_i - \hat{y}_i\| ;$$

(3) Apply the criterion for add rules:

if  $d_{\min} > k_d$ , and

$$E(x_i, u+1) = |a_{u+1}| \frac{R_{u+1}(x_i)}{\sum_{k=1}^{u+1} R_k(x_i)} > e_g$$

Allocate a new rule  $u+1$  with

$$a_{u+1} = e_n,$$

$$\mu_{u+1} = x_n,$$

$$\sigma_{u+1} = k \times d_{\min}.$$

else adjust the system parameters for the nearest rule only by using the EKF method [17].

$$E(\mathbf{x}_i, \min) = \left| a_{\min} \right| \frac{R_{\min}(x_i)}{\sum_{k=1}^u R_k(x_i)}$$

If  $E(\mathbf{x}_i, \min) < e_p$  Remove the  $i$ -th rule and reduce the dimensionality of EKF.

#### 4 FNN Model of AAC System

The development of the FNN model consists of four steps. The first step is acquiring experimental data from the AAC experimental rig; the second step is determination of a suitable FNN model for the AAC system, the third step is construction of the FNN model structure, and the final step is validation of the ANN model. Fig. 1 shows a schematic of the structure of the FNN model that was developed for the AAC system.

Parameter  $x$  represents the input signal;  $y$  represents the output signal from the model and  $e_i$  represents the error between the actual outputs  $y_i$  and the predicted outputs  $\hat{y}_i$ . The parameters  $n_c, T_{a,i,cond}, V_{a,i,evp}, T_{a,i,evp}$  act as the input data  $x$  in input. Then the data propagate to the second layer named fuzzy phase, and finally the output  $\hat{y}_i$  compared to the actual outputs  $y_i$ , the error is used to feedback the FNN till the target is achieved. The structure of air-condition system perform prediction based-FNN is illustratide by Fig. 2.

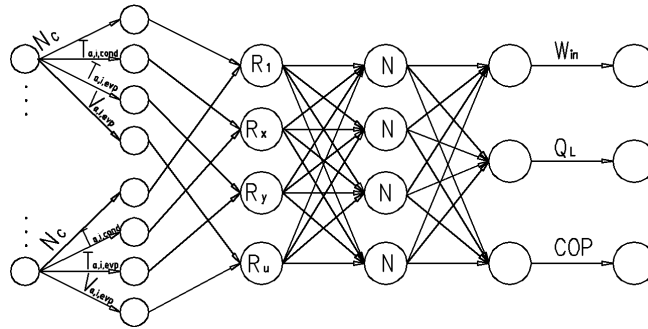


**Fig. 2.** The structure of air-condition prediction upon FNN

**Layer 1.** In layer1, each node represents an input variable and directly transmits the input signal to layer 2.

**Layer 2.** In this layer, each node represents the membership value of each input variable. FNN utilizes the equivalence between a RBF network and a FIS, then the antecedent part (if part) in fuzzy rules is achieved by Gaussian function of the RBF network. The membership value  $A_{ik}(x_i)$  of the  $i$ -th input variable  $x_i$  in the  $k$ -th Gaussian is given by

$$A_{ik}(x) = \exp\left(-\frac{(x_i - \mu_{ik})^2}{\sigma_k^2}\right) \quad k = 1, 2, \dots, u \quad (21)$$

where  $u$  the number of the Gaussian function is,  $\mu_{ik}$  is the center of the  $k$ -th Gaussian function for the  $i$ -th input variable,  $\sigma_k$  is the width of the  $k$ -th Gaussian function. In FNN, the width of all the input variables in the  $k$ -th Gaussian function is the same.

**Layer 3.** Each node in the layer represents the if part of if-then rules obtained by the sum-product composition and total number of such rules is  $u$ . The firing strength of the  $k$ -th rule is given by

$$R_k(x) = \prod_{i=1}^u A_{ik}(x_i) = \exp\left(-\sum_{i=1}^u \frac{(x_i - \mu_{ik})^2}{\sigma_k^2}\right) = \exp\left(-\frac{\|\mathbf{x} - \mu_k\|^2}{\sigma_k^2}\right) \quad (22)$$

where  $\mathbf{x} = (x_1, x_2, \dots, x_r) \in \mathcal{R}^r$ ,  $\mu_k = (\mu_{1k}, \mu_{1k}, \dots, \mu_{rk})$  is  $k$ -th RBF node.

**Layer 4.** Defuzzication layer, the nodes in the layer are named as nodes whose number is equal to the number of the nodes in third layer. The  $k$ -th normalized node is given by

$$\bar{R} = \frac{R_k(x)w_k}{\sum_{k=1}^u R_k(x)} \quad k = 1, 2, \dots, u \quad (23)$$

**Layer 5.** Output layer, each node in this layer corresponds to an output variable, which is given by the weighted sum of the output of each normalized rule. The system output is calculated by

$$\hat{y} = \sum_{k=1}^u a_k \bar{R}_k = \frac{\sum_{k=1}^u R_k(x)a_k}{\sum_{k=1}^u R_k(x)} \quad (24)$$

where  $\hat{y} = [\hat{y}_1, \hat{y}_2, \dots, \hat{y}_m]^T$  is the output of the system,  $a_k = [a_{1k}, a_{2k}, \dots, a_{mk}]^T$  is its connecting weight to the output neuron. The inputs to the FNN model is  $\mathbf{X}(x_1, x_2, x_3, x_4)$ ,  $x_1$  is compressor speed represented by  $N_{comp}$ ,  $x_2$  is air temperature at evaporator inlet represented by  $T_{a,i,evp}$ ,  $x_3$  is air temperatures at condenser inlet represented by  $T_{a,i,cond}$ ,  $x_4$  is air velocity at evaporator inlet  $V_{a,i,evp}$ . The output of the model is  $\mathbf{Y}(y_1, y_2, y_3)$ ,  $y_1$  is the cooling effect represented by  $Q_L$ ,  $y_2$  is the compressor input power represented by  $W$ ,  $y_3$  is the coefficient of performance (COP) of the system. The FNN model is developed through 2 stages: training stage and testing stage. The network is trained to predict an output based on input data during the training stage. To validate the result, the model is tested using difference sets of input. In this paper, we use MATLAB environment.

## 5 Model Validation

Statistical analysis is used to validate the performance of the FNN model, i.e. the correlation coefficient, mean relative error and root mean square. A correlation coefficient (R) is used to indicate the strength of the relationship between the predicted outputs  $\hat{y}$  and the actual outputs  $y$ . It is given by Ref. [18]

$$R = \frac{S_{y\hat{y}}}{\sqrt{S_{yy}S_{\hat{y}\hat{y}}}} \quad (25)$$

where  $S_{y\hat{y}}$ ,  $S_{yy}$ , and  $S_{\hat{y}\hat{y}}$  are respectively given by

$$S_{y\hat{y}} = \sum_{i=1}^n y_i \hat{y}_i - \frac{\left(\sum_{i=1}^n y_i\right)\left(\sum_{i=1}^n \hat{y}_i\right)}{n} \quad (26)$$

$$S_{yy} = \sum_{i=1}^n y_i^2 - \frac{\left(\sum_{i=1}^n y_i\right)^2}{n} \quad (27)$$

$$S_{\hat{y}\hat{y}} = \sum_{i=1}^n \hat{y}_i^2 - \frac{\left(\sum_{i=1}^n \hat{y}_i\right)^2}{n} \quad (28)$$

The mean square error (MAE) is other measures of FNN performance, root mean square error (RMSE) and error index (EI). The error index is defined as [19].

$$EI = \sqrt{\frac{\sum_{i=1}^n (y_i - \hat{y}_i)^2}{\sum_{i=1}^n y_i^2}} \quad (29)$$

## 6 Experimental Descriptions

Fig. 3 illustrates the schematic diagram of the AAC experimental rig in this study. It consists of three sections which are a vapor-compression refrigeration circuit, a closed air duct for evaporator section, and open air duct for condenser section respectively. The ducts are designed according to the British Standard for rating of duct mounted air cooling coils. Original components of a Denso air-conditioning system are used to construct the AAC system. The Denso air-conditioning system is used in a typical compact size car working with refrigerant R-134a. As seen in this figure, the main components of vapor compression refrigeration circuit consist of a swash-plate compressor, an evaporator, a condenser, an expansion valve, a receiver drier, a sight glass and insulated interconnecting pipes.

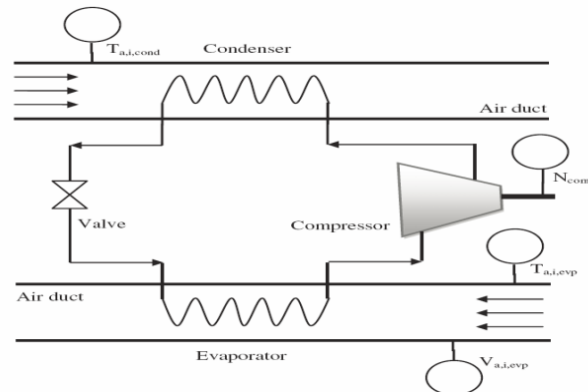


**Fig. 3.** Schematic diagram of the AAC system experimental rig

The air duct is a closed loop rectangular conduit whose overall length is 5130 mm. A 25mm thick rock wool material is used to thermally insulate the duct walls between the downstream and upstream of the evaporator coil. A variable speed centrifugal fan was used to force air to flow through the duct. To improve the air quality, we installed an air mixer, a honeycomb air flow straightener and gauge screens at the upstream location of the evaporator coil. A 2 KW electrical heater was used to the evaporator coil. To alter the humidity of the air, the ducting system was incorporated with a steam humidifier to inject vapor at a rate of 4 kg/h into the air stream. The air temperature and humidity at the evaporator coil inlet was adjusted using the heating and humidification sections. The air duct of the condenser is an open rectangular conduit whose length is 663 mm. In order to let air flow through the duct, a constant speed blower was installed at the upstream location of the air duct. A reducer unit and damper was used to control the blower speed so as to change the velocity of the air passing through the condenser. A 2 KW electrical heater was used to change the dry-bulb temperature of the air at the inlet to the condenser coil.

The AAC experimental rig was furnished with data acquisition system which is consisted of a standard notebook computer with a personal computer memory card international association (PCMCIA) slot, a data acquisition PCMCIA card and a signal conditioning rack. We use two pt100 resistance temperature detector (RTD) sensors to measure the air temperature at the upstream and downstream locations of the evaporator coil. To measure the air temperature at the upstream of the condenser coil, another pt100 RTD sensor was used. Velocity of the air flowing through the evaporator and condenser coils was measured using two air velocity transducers. The compressor speed was regulated using a frequency inverter. Type-k thermocouples that were inserted into the copper tubing were used to measure the temperature of the refrigerant at various locations in the vapor-compression refrigeration circuit.

A Bourdon tube pressure gauge was used to measure the pressure at the compressor suction and discharge sections. It was assumed that there was no pressure loss in the piping hence the condensing and evaporating pressures are equal to the suction and discharge pressures, respectively. A flow meter which was mounted at the exit of the condenser was used to measure the mass flow rate of the refrigerant. A sight glass tube was placed before the flow meter to ensure that the refrigerant is always in a sub-cooled state. Some features of the instrumentation are summarized in Table 1.

**Table 1.** Characteristics of the instrumentation

Measured variable	Instrument	Range	Uncertainty
Temperature	RTD sensors	-25°C~100°C	±0.3°C
Pressure	Bourdon gauge	0~300kPa	±1kPa
Humidity	Humidity sensors	0~100%RH	±1%
Air velocity	Velocity transducer	0~20m/s	±0.5%
Mass flow rate	Flow meter	0~25kg/s	±1%
Compressor speed	Digital tachometer	0~20000rpm	±2%
Voltage	Digital voltmeter	0~250V	±1%
Current	Digital ammeter	0~20A	±1%

During the experiments, the AAC system was run until a steady-state condition was attained. During series of experiments, four operating parameters were varied, each with their respective range as shown below. The condenser air velocity was held constant at about 1.6 m/s at all time.

Evaporator inlet air dry-bulb temperature,  $T_{a,i,evp}$  25 – 35°C .

Condenser inlet air dry-bulb temperature,  $T_{a,i,cond}$  32 – 40°C .

Compressor speed,  $N_{comp}$  1500 – 2500rpm .

Evaporator air velocity,  $V_{a,i,evp}$  1.6 – 3.8m/s .

The tests were run at different compressor speeds with varying evaporator heat load. In the air side tests, the compressor speed was set at 1500, 2000, and 2500 rpm by controlling the motor speed using a frequency inverter. At each compressor speed, the air velocity of the evaporator coil is maintained at the blower speeds 1, 2, 3 and 4. At each blower speed, the air dry-bulb temperature at the inlet of the evaporator was kept at 25, 30 and 35°C by varying the electrical energy input to the electric heater. At each evaporator inlet air temperature, the air dry-bulb temperature at the inlet of the condenser was set at 32, 35 and 40°C, by varying the electrical energy input to the electric heaters. To stabilize the AAC system, the air-conditioner was run 30 min prior to each test, the cooling capacity, i.e. the rate of heat removal in the evaporator  $Q_L$ , compressor power input W and the coefficient of performance (COP) of the AAC system were determined.

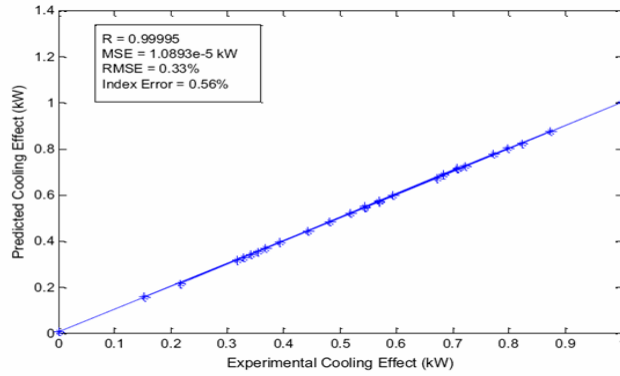
A parametric study is conducted to investigate the effects of different data types, input parameters and the number of rules on the performance of the FNN model of the AAC system. During the study the output results are predicted by the model in comparison with the results derived from the experiments. About 70% of the data is used for training and the remaining for prediction of the FNN model. The performance is assessed by determining the average values of the mean square error(MSE), the root mean square error(RMSE) and the error index (EI). During the training process the weighting coefficients are adjusted by using the EKF method.

## 7 Experimental Results and Discussions

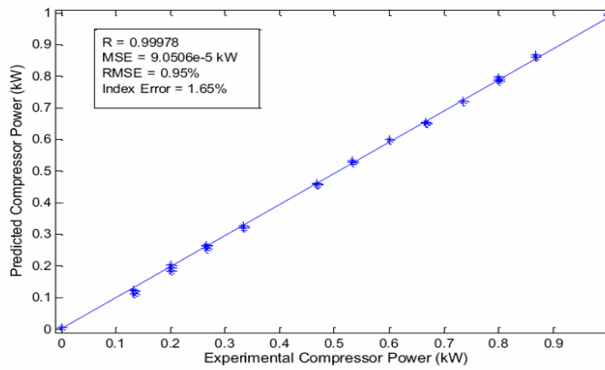
During this study the output results predicted by the model were compared with the results obtained from the experiments. About 70% of the data was dedicated for training and remaining for capability prediction of the FNN model. The performance was assessed by determining the average values of the mean square error (MSE), the root mean square error (RMSE), and the error index (EI). During the training process the weighing coefficient were adjusted by using extended Kalman filter (EKF) algorithm.

Fig. 4 to Fig. 6 are the plots of performance of the AAC system predicted by the FNN model vs. the corresponding values obtained from experiments. Note that in all cases, the correlation coefficients R are very close to unity. This indicates that the FNN model was able to predict the performance parameters of the AAC system with a very good accuracy. As shown in Fig. 4, the plot of cooling effects predicted by the FNN model vs. the values obtained from the experiments. The FNN predictions yield a mean square error (MSE) of about  $1.09 \times 10^{-5}$ kw, root mean square error (RMSE) of 0.33%, error index of 0.56% and correlation coefficient, R of 0.99. These values show that the FNN model is able to predict the heat absorbed by the refrigerant in the evaporator with a very good accuracy. A plot of the FNN prediction of the compressor power vs. the experimental values is shown in Fig. 6. The FNN prediction produces MSE value of about  $9.05 \times 10^{-5}$ KW, RMSE of 0.95%, index error of 1.65% and correlation coefficient of

0.9998. Fig. 7 shows the plot of coefficient of performance (COP) of the AAC system predicted by the FNN model vs. the values obtained from the experiments. The FNN prediction yields MSE value of about  $7.28 \times 10^{-5}$ , RMSE of 0.85%. Index error of 1.65% and correlation coefficient R of 0.9997. Note that predicted results are well close to the experimental data and the deviations are small for each performance parameter. Fig. 7 shows plots of the predicted vs. actual outputs for this optimized FNN model for both training and test data sets. The graph shows a close agreement between the outputs of FNN model and actual experimental data.



**Fig. 4.** FNN prediction of the cooling effect vs. the experimental results



**Fig. 5.** FNN prediction of the compressor power vs. the experimental results

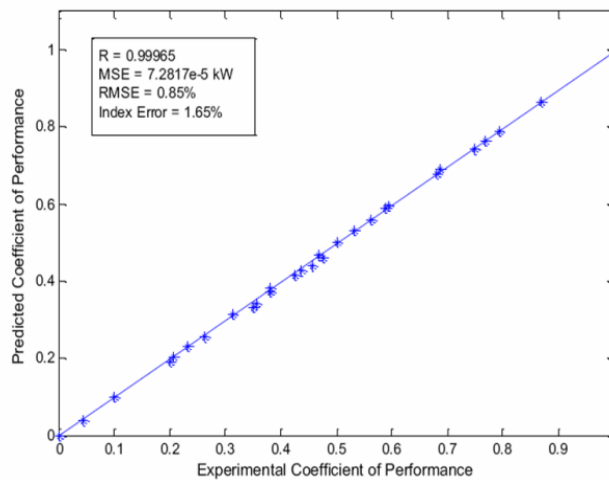


**Fig. 6.** FNN prediction of the coefficient of performance vs. the experimental results

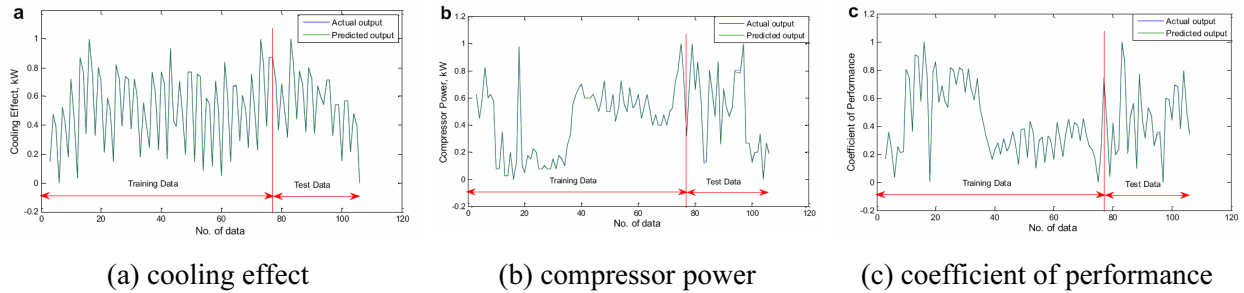


**Fig. 7.** The actual and predict output

## 8 Conclusions

In this paper a Fuzzy neural network (FNN) based on the functional equivalence between a RBF and a FIS has been developed to predict the performance parameters of an experimental AAC system. The FNN model contains five layers. Training and testing data set for the FNN model were obtained from steady state tests conducted on the AAC experimental rig. The cooling load, compressor power input and the coefficient of performance of the AAC system experimental rig are predicted using the trained FNN model. The mean square error, root mean square error, error index and the correlation coefficient were used to assess the performance of the FNN model. From the result of the experiments, the FNN model was found to be capable of accurately predicting the performance parameters of the AAC system. All performance parameters are found to be very close to unity so that it indicates that the FNN model can predict the performance parameters of the AAC system with a very good accuracy.

## Acknowledgements

This work was supported in part by Fujian Provincial Department of Science and Technology, Granted No. 2017J01729 and No. 2017037, and Science Research of Education Department of Hunan Province (No. 17C0010).

## References

- [1] ASHRAE, 2008 Ashrae Handbook: HVAC Systems and Equipment, ASHRAE, Atlanta, 2008.
- [2] R.L. Navale, R.M. Nelson, Use of genetic algorithms and evolutionary strategies to develop and adaptive fuzzy logic controller for a cooling coil: comparison of the AFLC with a standard PID controller, *Energy & Buildings* 45(1)(2011) 169-180.
- [3] N. Etik, N. Allahverdi, I.U. Sert, I. Saritas, Fuzzy expert system design for operating room air-condition control systems, *ExpertSyst. Appl.* 36(2009) 9753-9758.
- [4] A. Kargilis, Design and Development of Automotive Air Conditioning Systems, ALKAR Engineering Company, Southfield, 2003.
- [5] P.J. Rubas, C.W. Bullard, Factors contributing to refrigerator cycling losses, *International Journal of Refrigeration* 18(3)(1995) 168-176.
- [6] E.B. Ratts, J.S. Brown, An experimental analysis of the effect of the refrigerant charge level on an automotive refrigeration system, *International Journal of Thermal Science* 39(2000) 592-604.
- [7] O.M. Al-Rabghi, A.A. Niyaz, Retrofitting R-12 car air conditioner with R-134a refrigerant, *International Journal of Energy Research* 24(2000) 467-474.

- [8] O. Kaynakli, I. Horuz, An experimental analysis of automotive air conditioning system, *International Communications in Heat and Mass Transfer* 30(2003) 273-284.
- [9] M. Hosoz, M. Direk, Performance evaluation of an integrated automotive airconditioning and heat pump system, *Energy Conversion and Management* 47(2006) 545-559.
- [10] H.M. Kamar, R. Ahmad, N.B. Kamsah, A.F.M. Mustafa, Artificial neural networks for automotive air-conditioning systems performance prediction, *Applied Thermal Engineering* 50(1)(2013) 63-70.
- [11] Y.-C. Chang, Sequencing of chillers by estimating chiller power consumption using artificial neural networks, *Building and Environment* 42(2007) 180-188.
- [12] H.M. Ertunc, M. Hosoz, Comparative analysis of an evaporative condenser using artificial neural network and adaptive neuro-fuzzy inference system, *International Journal of Refrigeration* 31(2008) 1426-1436.
- [13] M. Mohanraj, S. Jayaraj, C. Muraleedharan, Applications of artificial neural networks for refrigeration, air-conditioning and heat pump systems -a review, *Renewable and Sustainable Energy Reviews* 16(2012) 1340-1358.
- [14] A.H. Attia, S.F. Rezek, A.M. Saleh, Fuzzy logic control of air-conditioning system in residential buildings, *AEJ-Alexandria Engineering Journal* 36(3)(2015) 395-403.
- [15] N. Li, L. Xia, D. Shiming, X. Xu, M.Y. Chan, On-line adaptive control of a direct expansion air conditioning system using artificial neural network, *Applied Thermal Engineering* 53(1)(2013) 96-107.
- [16] H. Rong, X. Ye, X. Xiang, A self adaptive incremental learning fuzzy neural network based on the influence of a fuzzy rule, in: *Proc. International Conference on Intelligent Information Hiding and Multimedia Signal Processing*, 2015.
- [17] R. Hu, Y. Sha, H.Y. Yang, A Novel Uninorm-Based Evolving Fuzzy Neural Networks, in: A. Abraham, X. Jiang, V. Snášel, J.S. Pan (Eds.), *Intelligent Data Analysis and Applications: Advances in Intelligent Systems and Computing*, vol. 370, Springer, Cham, 2015, pp. 469-478.
- [18] M.T. Hagan, H.B. Demuth, M. Beale, *Neural Network Design*, PWS, Boston, 1995.
- [19] R. Ahmad, H. Jamaluddin, M.A. Hussain, Application of memetic algorithm in modelling discrete-time multivariable dynamics systems, *Mechanical Systems and Signal Processing* 22(2008) 1595-1609.
- [20] H.-J. Rong, S. Han, J.-M. Bai, Y.-Q. Liang, Improved adaptive control for wing rock via fuzzy neural network with randomly assigned fuzzy membership function parameters, *Original Research Article Aerospace Science and Technology* 39(2014) 614-627.
- [21] J.P. Rugh, T.J. Hendricks, *Effect of Solar Reflective Glazing on Ford Explorer Climate Control, Fuel Economy, and Emissions*, Society of Automotive Engineers (SAE), Warrendale, 2001.
- [22] H. Nasution, M.N.W. Hassan, Potential electricity savings by variable speed control of compressor for air conditioning systems, *Clean. Technol. Environ. Policy* 8(2006) 105-111.
- [23] L.O.S. Buzelin, S.C. Amico, J.V.C. Vargas, J.A.R. Parise, Experimental development of an intelligent refrigeration system, *Int. J. Refrig.* 28(2005) 165-175.
- [24] S.A. Tassou, T.Q. Qureshi, Performance of a variable-speed inverter motor drive for refrigeration applications, *Computer Control Eng. J.* 5 (1994) 193-199.
- [25] O. Sirch, 48 Volt and its threats and opportunities, in: *Proc. Automotive 48 Volt Power Supply System*, 2013.
- [26] J. Zhang, G. Qin, B. Xu, H. Hu, Z. Chen, Study on automotive air conditioner control system based on incremental-PID, *Adv. Mater. Res.* 129-131(2010) 17-22.
- [27] B.C. Ng, I.Z.M. Darus, H.M. Kamar, M. Norazlan, Dynamic modeling of an automotive air conditioning system and an

- auto tuned PID controller using extremum seeking algorithm, in: Proc. IEEE Symposium on Computers & Informatics, 2013.
- [28] B.C. Ng, I.Z.M. Darus, H. Jamaluddin, H.M. Kamar, Dynamic modelling of an automotive variable speed air conditioning system using nonlinear autoregressive exogenous neural networks, *Appl. Therm. Eng.* 73(2014) 1255-1269.
- [29] X.-D. He, S. Liu, H. Asada, Modeling of vapor compression cycles for multivariable feedback control of HVAC systems, *J. Dyn. Syst. Meas. Control* 119(1997) 183-191.
- [30] L.C. Schurt, C.J.L. Hermes, A.T. Neto, A model-driven multivariable controller for vapor compression refrigeration systems, *Int. J. Refrig.* 32(2009) 1672-1682.
- [31] B. Rasmussen, Control-oriented modeling of transcritical vapor compression systems, ATRC-TR 204, 2002.
- [32] D. Leducq, G. Guilpart, G. Trystram, Low order dynamic model of a vapour compression cycle for food process control design, *J. Food Process Eng.* 26(2003) 67-91.
- [33] K. Hornik, H.W. Stinchcombe, Multilayer feedforward networks are universal approximators, *Neural Networks* 2(1989) 359-366.
- [34] K.S. Narendra, K. Parthasarathy, Identification and control of dynamical system using neural networks, *IEEE Transaction on Neural Networks* 1(1)(1990) 4-27.